An Evaluation on Radiation Shielding and Activation Properties of ISOL-bunker Structural Materials for Radiation Safety in RAON Accelerator

Do Hyun KIM [a], Song Hyun KIM [a], Myeong Hyeon WOO [a], Jae Yong LEE [a], Jong Woo KIM [a], Chang Ho SHIN [a,*], and Shin Woo NAM [b]

[a]*Department of Nuclear Engineering, Hanyang University, Seoul, Korea, 133-791*
[b]*Institute for Basic Science, 1689 Yuseong-daero, Yuseong-gu, Daejeon, Korea, 305-811*
[*]*Corresponding author: gemini@ hanyang.ac.kr*

1. Introduction

RAON heavy ion accelerator has been designed by the Institute for Basic Science (IBS) [1]. ISOL is one of RAON facilities to generate and separate rare isotopes. For generating rare isotopes, high intensity proton beam, which has 70 MeV energy, is induced into UCx target. From this reaction, lots of neutrons are concomitantly generated. In our previous study [2-3], prompt radiation shielding and activation analysis were performed for ISOL-bunker (target room) using concrete. However, those results showed that residual dose from activated concrete were highly evaluated than our design goal. Therefore, to meet our design goal, it was required that the structural material of ISOL-bunker should be carefully selected. In this study, to select the structural material which has lower activation property with higher performance for radiation shielding, following aspects were evaluated: (i) residual dose, (ii) radioactive wastes, and (iii) shielding performance in ISOL-bunker.

2. Methods and Results

Fig.1 is the radial view of ISOL-bunker. The UC_2 target which has 3.77 cm height and 6 cm diameter is located at T. The maximum proton beam is 70 kW (70 MeV proton with 1 mA current). In our previous study [3], the main radiation to be considered for the radiation safety was secondary neutrons generated from proton induced target reaction.

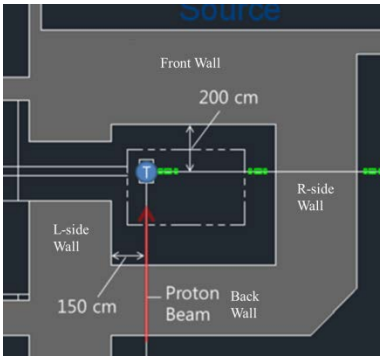

Fig. 1. Radial View of ISOL-bunker

It is well known that residual gamma sources were mainly produced by transmutation of impurities in the concrete as the ISOL structure, which are ^{6}Li, ^{59}Co, ^{58}Ni, ^{62}Ni, ^{133}Cs, ^{151}Eu, and ^{153}Eu [2, 4-6]. In this study, to reduce the residual radiations generated by activated concrete, two temporal strategies are proposed; (#1) to replace the normal concrete to specific concretes; (#2) to design dual-layer radiation shields that a specific shielding material is located inner side of the normal concrete.

To realize #1 strategy, specific concretes containing hematite, magnetite, or colemanite [7-9] as given in Table I were used instead of the normal concrete. Also, to design the shielding with #2 strategy, the shielding materials given in Table II were used that have 20 cm, 40 cm, and 60 cm thicknesses, respectively. For the calculation, the normal concrete composition, which was used in previous study, was used. The composition of the normal concrete is given in Table III.

Table I: Information of Shielding Materials for #1 Strategy

Hematite (50 wt%) Containing Concrete (2.7 g/cm^2)			
Nuclide	Weight Raito	Nuclide	Weight Raito
H*	2.895E-03	Mn*	5.601E-04
O*	4.100E-01	Ti*	1.162E-04
Na*	8.908E-03	^{6}Li	1.351E-06
Mg*	6.164E-03	^{59}Co	6.641E-06
Al*	2.539E-02	^{58}Ni	1.959E-05
Si*	1.754E-01	^{62}Ni	1.535E-06
K*	1.002E-02	^{133}Cs	1.796E-06
Ca*	6.092E-02	^{151}Eu	6.289E-07
Fe*	2.996E-01	^{153}Eu	6.889E-07
Magnetite (50 wt%) Containing Concrete (2.7 g/cm^2)			
H*	2.771E-03	Cu*	5.193E-05
O*	3.749E-01	Ba*	1.003E-02
Na*	9.249E-03	^{6}Li	1.390E-06
Mg*	2.787E-03	^{59}Co	6.834E-06
Al*	2.614E-02	^{58}Ni	2.016E-05
Si*	1.778E-01	^{62}Ni	1.580E-06
K*	9.590E-03	^{133}Cs	1.849E-06
Ca*	4.546E-02	^{151}Eu	6.472E-07
Fe*	3.395E-01	^{153}Eu	7.089E-07
Mn*	1.704E-03	-	-
Colemanite (22 wt%) Containing Concrete (2.3 g/cm^2)			
H*	4.655E-03	Fe*	1.106E-02
B*	2.815E-02	^{6}Li	2.168E-06
O*	5.046E-01	^{59}Co	1.066E-05
Na*	1.432E-02	^{58}Ni	3.144E-05
Mg*	4.033E-03	^{62}Ni	2.465E-06
Al*	3.831E-02	^{133}Cs	2.884E-06
Si*	2.709E-01	^{151}Eu	1.010E-06
K*	1.611E-02	^{153}Eu	1.106E-06
Ca*	1.078E-01	-	-

* Natural Nuclide

Table II: Information of Shielding Materials for #2 Strategy

B_4C (2.52 g/cm^2)			
Nuclide	Weight Raito	Nuclide	Weight Raito
B*	7.826E-01	C*	2.174E-01
Borosilicate Glass (2.23 g/cm^2)			
B*	4.006E-02	O*	5.396E-01
Na*	2.819E-02	Al*	1.164E-02
Si*	3.772E-01	K*	3.321E-03
Carbon (1.8 g/cm^2)			
C*	1.000E+00	-	-
Polyethylene (0.92 g/cm^2)			
H*	1.437E-01	C*	8.563E-01
Borated Polyethylene (1.00 g/cm^2)			
H*	1.254E-01	C*	7.746E-01
B*	1.000E-01	-	-

* Natural Nuclide

Table III: Composition of Normal Concrete for Activation Calculations [2]

Nuclide	Weight Raito	Nuclide	Weight Raito
H*	5.532E-03	O*	4.983E-01
Si*	3.157E-01	Ca*	8.255E-02
Na*	1.702E-02	Mg*	2.553E-03
Al*	4.553E-02	S*	1.277E-03
K*	1.915E-02	Fe*	1.234E-02
^{6}Li	2.776E-06	^{133}Cs	3.693E-06
^{59}Co	1.365E-05	^{151}Eu	1.293E-06
^{58}Ni	4.026E-05	^{153}Eu	1.416E-06
^{62}Ni	3.156E-06	^{133}Cs	3.693E-06

* Natural Nuclide

For activation evaluation, rigorous-two-step (R2S) method [10] was used by coupling the particle transport code and activation code as following step:

(i) Neutron spectra and spallation information, which are recoded from over 20 MeV neutron reactions, are estimated by particle transport calculation.
(ii) Amount of isotope and gamma source information are calculated by activation code.
(iii) Residual dose is simulated by particle transport code using gamma source information from step (ii).

For simulation of particle transport, MCNPX 2.7 code [11] was used with JENDL/HE 2007 nuclear library. The activation calculation was performed by SP-FISPACT 2010 [12-13]. To apply R2S method, large and dense material should be divided to sub-regions. In our previous study [2], the length of the sub-region, which does not significantly affect the activation results, was evaluated to 20 cm. Thus, ISOL-bunker geometry to estimate the activations was modeled as shown Fig.2.

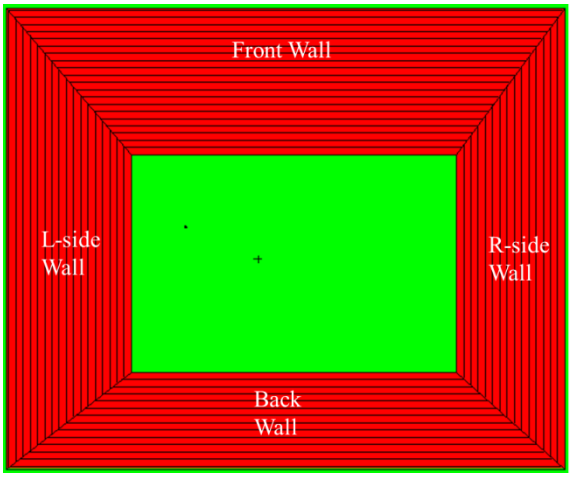

(a) #1 strategy

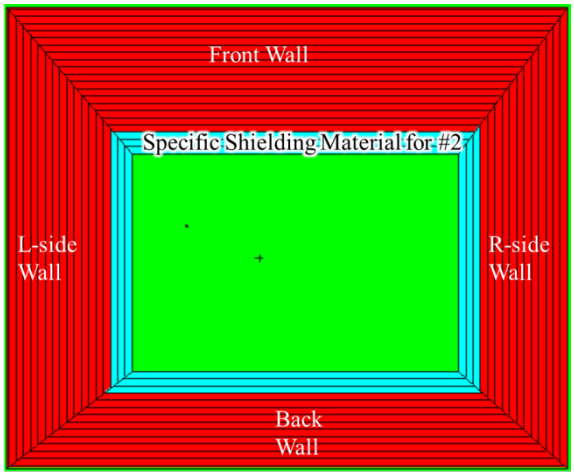

(b) #2 Strategy

Fig. 2. Geometry Modeling for Proposed Strategy

2.1 Residual Dose Analysis

To perform the activation analysis, operating plan was assumed to 30 years. During the activation period, 14 day irradiation and 14 day decay were repeated.

Table IV and Fig. 3 are results according to decay time after operating period using the specific concretes given in Table I. All results were represented to the maximum doses in the ISOL-bunker. The residual radiations using hematite, magnetite, and colemanite concretes were decreased about 39 %, 36 %, and 89 % compared to the normal concrete, respectively.

Table V and Fig. 4 are results of the residual doses using #2 strategy. As using the B_4C, Borated Polyethylene, and Polyethylene, the residual doses were significantly reduced compared to normal concrete. Hence, compared to the #1 strategy, this shows better performance to reduce the residual doses.

Table IV: Residual Dose using Various Shielding Material Based on Concrete after 30 Year Operating Period

	Maximum Dose (uSv/hr) in ISOL-bunker			
Decay Time	Normal Concrete	Colemanite Concrete	Hematite Concrete	Magnetite Concrete
0 Day	1.05E+06	1.43E+05	3.67E+05	4.57E+05
1 Day	2.76E+05	7.87E+03	6.84E+04	6.56E+04
7 Day	2.11E+04	2.30E+03	1.40E+04	1.49E+04
30 Day	2.05E+04	2.22E+03	1.25E+04	1.31E+04
90 Day	2.00E+04	2.10E+03	1.05E+04	1.09E+04
180 Day	1.95E+04	1.95E+03	8.91E+03	9.22E+03
1 Year	1.87E+04	1.70E+03	7.16E+03	7.30E+03
5 Year	1.39E+04	6.72E+02	3.17E+03	3.00E+03
10 Year	1.00E+04	2.59E+02	2.12E+03	1.99E+03

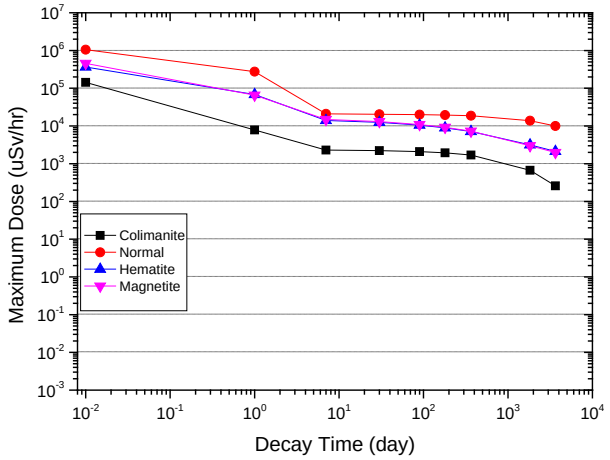

Fig. 3. Residual Dose using Strategy #1 after 30 Year Operating Period According to Decay Time

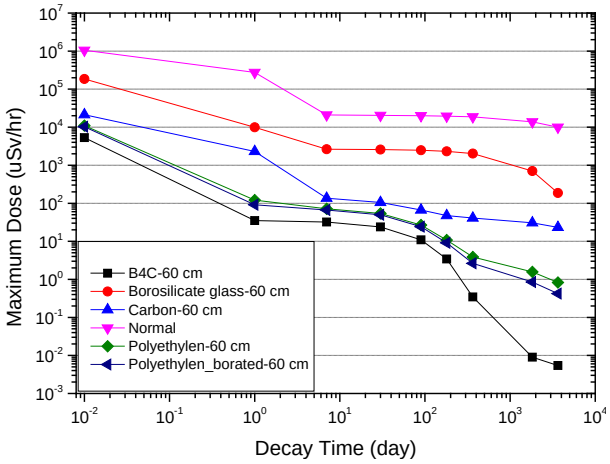

Fig. 4 Residual Dose using Strategy #1 (60 cm) with Normal Concrete after 30 Year Operating Period According to Decay Time

Table V: Residual Dose using Various Added Shielding Material with Normal Concrete after 30 Year Operating Period

	Maximum Dose (uSv/hr)																	
Decay Time	B4C			Borosilicate Glass			Carbon			Polyethylene			Borated Polyethylene					
	20 cm	40 cm	60 cm	20 cm	40cm	60 cm	20 cm	40 cm	60 cm	20 cm	40 cm	60 cm	20 cm	40 cm	60 cm			
0 Day	9.54E+03	5.43E+03	5.30E+03	2.08E+05	1.86E+05	1.85E+05	2.25E+05	5.04E+04	2.13E+04	3.73E+04	1.28E+04	1.10E+04	2.37E+04	1.15E+04	1.03E+04			
1 Day	9.30E+02	5.85E+01	3.51E+01	1.81E+04	1.03E+04	9.96E+03	6.55E+04	1.27E+04	2.31E+03	5.87E+03	4.23E+02	1.21E+02	1.89E+03	2.28E+02	9.14E+01			
7 Day	8.65E+01	3.54E+01	3.21E+01	3.10E+03	2.67E+03	2.63E+03	3.10E+03	4.02E+02	1.36E+02	5.23E+02	9.97E+01	7.17E+01	2.97E+02	8.58E+01	6.63E+01			
30 Day	7.60E+01	2.49E+01	2.39E+01	3.04E+03	2.61E+03	2.58E+03	2.98E+03	3.74E+02	1.05E+02	4.96E+02	8.18E+01	5.40E+01	2.76E+02	6.83E+01	4.99E+01			
90 Day	6.34E+01	1.18E+01	1.09E+01	2.92E+03	2.51E+03	2.47E+03	2.90E+03	3.39E+02	6.66E+01	4.57E+02	5.31E+01	2.69E+01	2.43E+02	4.16E+01	2.41E+01			
180 Day	5.44E+01	4.15E+00	3.43E+00	2.75E+03	2.34E+03	2.31E+03	2.83E+03	3.19E+02	4.75E+01	4.28E+02	3.62E+01	1.08E+01	2.17E+02	2.56E+01	9.10E+00			
1 Year	4.83E+01	8.42E-01	3.44E-01	2.43E+03	2.05E+03	2.02E+03	2.71E+03	3.00E+02	4.10E+01	3.92E+02	2.69E+01	3.88E+00	1.90E+02	1.72E+01	2.64E+00			
5 Year	2.93E+01	2.95E-01	9.02E-03	9.75E+02	7.15E+02	7.02E+02	2.06E+03	2.31E+02	3.07E+01	2.47E+02	1.37E+01	1.57E+00	9.30E+01	7.42E+00	8.52E-01			
10 Year	1.85E+01	1.59E-01	5.42E-03	3.63E+02	1.94E+02	1.87E+02	1.50E+03	1.70E+02	2.33E+01	1.62E+02	7.71E+00	8.30E-01	5.03E+01	3.48E+00	4.23E-01			

2.2 Radioactive Waste Analysis

Nowadays, radioactive waste from decommissioning of radiation facility has been issued. After 30 year operating, RAON accelerator is planned to be decommissioned; therefore, amount of radioactive waste should be properly considered at the beginning of the design step. In Korea regulation, the radioactive wastes, which must be deposited at radioactive waste disposal site, are classified by using following equation:

$$\begin{cases} \sum_i \frac{C_i}{C_{L,i}} \geq 1, \ Radioactive\ Waste \\ \sum_i \frac{C_i}{C_{L,i}} < 1, \ Normal\ Waste \end{cases} \quad (1)$$

where C_i is activity of ith nuclide, and $C_{L,i}$ is permissible concentration given in Table VI.

Table VI: Permissible Concentration of Radionuclide Activity in Korea Regulation

Radio Nuclide	Permissible Concentration (Bq/g)
I-129	0.01
Na-22, Sc-46, Mn-54, Co-56, Co-60, Zn-65, Nb-94, Ru-106, Ag-110m, Sb-125, Cs-134, Cs-137, Eu-152, Eu-154, Ta-182, Bi-207, Th-229, U-232, Pu-238, Pu-239, Pu-240, Pu-242, Pu-244, Am-241, Am-242m, Am-243, Cm-245, Cm-246, Cm-247, Cm-248, Cf-249, Cf-251, Es-254	0.1
C-14, Na-24, Cl-36, Sc-48, V-48, Mn-52, Fe-59, Co-57, Co-58, Se-75, Br-82, Sr-85, Sr-90, Zr-95, Nb-95, Tc-96, Tc-99, Ru-103, Ag-105, Cd-109, Sn-113, Sb-124, Te-123m, Te-132, Cs-136, Ba-140, La-140, Ce-139, Eu-155, Tb-160, Hf-181, Os-185, Ir-190, Ir-192, Tl-204, Bi-206, U-233, Np-237, Pu-236, Cm-243, Cm-244, Cf-248, Cf-250, Cf-252, Cf-254	1
Be-7, F-18, Cl-38, K-43, Ca-47, Mn-51, Mn-52m, Mn-56, Fe-52, Co-55, Co-62m, Ni-65, Zn-69m, Ga-72, As-74, As-76, Sr-91, Sr-92, Zr-93, Zr-97, Nb-93m, Nb-97, Nb-98, Mo-90, Mo-93, Mo-99, Mo-101, Tc-97, Ru-97, Ru-105, Cd-115, In-111, In-114m, Sn-125, Sb-122, Te-127m, Te-129m, Te-131m, Te-133, Te-133m, Te-134, I-126, I-130, I-131, I-132, I-133, I-134, I-135, Cs-129, Cs-132, Cs-138, Ba-131, Ce-143, Ce-144, Gd-153, W-181, W-187, Pt-191, Au-198, Hg-203, Tl-200, Tl-202, Pb-203, Po-203, Po-205, Po-207, Ra-225, Pa-230, Pa-233, U-230b, U-236, Np-240, u-241, Cm-242, Es-254m	10
H-3, S-35, K-42, Ca-45, Sc-47, Cr-51, Mn-53, Co-61, Ni-59, Ni-63, Cu-64, Rb-86, Sr-85m, Sr-87m, Y-91, Y-91m, Y-92, Y-93, Tc-97m, Tc-99m, Rh-105, Pd-109, Ag-111, Cd-115m, In-113m, In-115m, Te-129, Te-131, I-123, I-125,Cs-135, Ce-141, Pr-142, Nd-147, Nd-149, Sm-153, Eu-152m, Gd-159, Dy-166, Ho-166, Er-171, Tm-170, Yb-175, Lu-177, Re-188, Os-191, Os-193, Ir-194, Pt-197m, Au-199, Hg-197, Hg-197m, Tl-201, Ra-227, U-231, U-237, U-239, U-240, Np-239, Pu-234, Pu-235, Pu-237, Bk-249, Cf-253, Es-253, Fm-255	100
Si-31, P-32, P-33, Fe-55, Co-60m, Zn-69, As-73, As-77, Sr-89, Y-90, Tc-96m, Pd-103, Te-125m, Te-127, Cs-131, Cs-134m, Pr-143, Pm-147, Pm-149, Sm-151, Dy-165, Er-169, Tm-171, W-185, Re-186, Os-191m, Pt-193m, Pt-197, At-211, Th-226, Pu-243, Am-242, Cf-246	1,000
Co-58m, Ge-71, Rh-103m, Fm-254	10,000

Table VII and Fig. 5 are result of radioactive waste after 30 year operating period with 1 year decay time. Analysis shows that the proposed strategies cannot effectively reduce the amount of the radioactive wastes for the front wall; however, colemanite concrete and B_4C shielding show that it can partially reduce the amount of the radioactive.

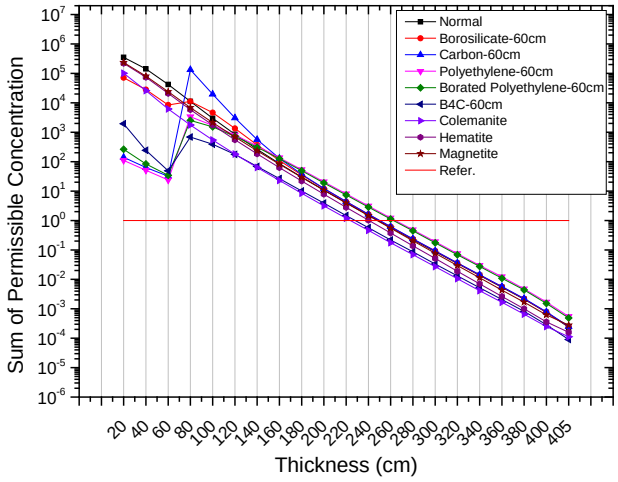

Fig. 5. Total Concentration of Radioactive Wastes for Each Thickness in Front Wall

Table VII: Required Thickness to Be Disposed after 30 Year Operations with 1 Year Decay Time

[unit: cm]

Shielding Material	Front	R-side	Back	L-side	Roof	Bottom
Normal	260	180	200	200	200	200
Colemanite	240	160	160	180	160	180
Hematite	260	160	180	200	180	200
Magnetite	260	180	180	200	180	200
Borosilicate (20 cm)	260	180	200	220	200	200
Borosilicate (40 cm)	260	200	200	220	200	220
Borosilicate (60 cm)	260	200	200	220	200	220
Carbon (20 cm)	260	180	200	200	200	200
Carbon (40 cm)	260	200	200	200	200	200
Carbon (60 cm)	260	200	200	220	200	220
Polyethylene (20 cm)	260	180	180	200	180	200
Polyethylene (40 cm)	260	160	160	200	180	200
Polyethylene (60 cm)	280	160	160	200	180	200
Borated Polyethylene (20 cm)	260	180	180	200	180	200
Borated Polyethylene (40 cm)	260	160	160	200	180	200
Borated Polyethylene (60 cm)	280	160	160	200	180	200
B_4C (20 cm)	260	160	180	200	180	200
B_4C (40 cm)	240	160	160	180	160	180
B_4C (60 cm)	240	140	140	180	140	160

2.3 Shielding Performance Analysis

Main function of ISOL-bunker radiation shielding is to protect the secondary radiations generated from target reaction with 70 MeV protons. Therefore, shielding performance of the shielding material with the proposed strategies should be confirmed. In this section, shielding performances with the proposed methods were evaluated for the prompt neutron. Fig. 6 shows dose results according to shielding depth. And, Table VI gives dose rate at the end of front wall (380 cm). The results show that the thickness to protect the radiation hazard is reduced about 20 cm when hematite and magnetite containing concretes and B_4C shielding are used.

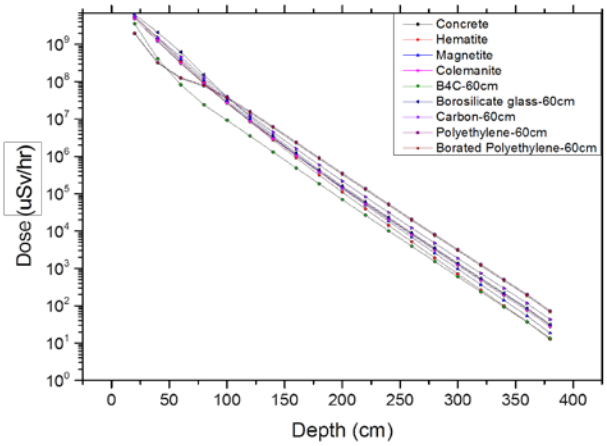

Fig. 6 Dose Distribution in Considered Shielding Materials According to Shielding Depth

Table VII: Dose Rate at End of Front Shielding Using Considered Shielding Materials

Shielding Material	Dose	Relative Error
Normal	1.26E+01	0.0185
Colemanite	1.17E+01	0.0163
Hematite	4.94E+00	0.022
Magnetite	7.19E+00	0.0183
Borosilicate (20 cm)	1.30E+01	0.0228
Borosilicate (40 cm)	1.28E+01	0.0191
Borosilicate (60 cm)	1.33E+01	0.0191
Carbon (20 cm)	1.42E+01	0.0161
Carbon (40 cm)	1.51E+01	0.0188
Carbon (60 cm)	1.80E+01	0.0204
Polyethylene (20 cm)	1.79E+01	0.0182
Polyethylene (40 cm)	2.32E+01	0.0224
Polyethylene (60 cm)	3.13E+01	0.0267
Borated Polyethylene (20 cm)	1.71E+01	0.0214
Borated Polyethylene (40 cm)	2.16E+01	0.0531
Borated Polyethylene (60 cm)	2.92E+01	0.0446
B_4C (20 cm)	9.80E+00	0.0222
B_4C (40 cm)	7.98E+00	0.052
B_4C (60 cm)	5.49E+00	0.0262

3. Conclusions

In this study, to effectively design the radiation shielding of the RAON ISOL-bunker, two methods were proposed. #1 strategy is a method to replace the normal concrete to specific concretes. #2 strategy is to design dual-layer radiation shields that a specific shielding material is located inner side of the normal concrete. Using the strategies, performance evaluations were evaluated for three aspects, which are residual dose, radioactive waste, and prompt radiation. The results show that the residual radiation can be effectively reduced using B_4C, borated polyethylene and polyethylene with #2 strategy. Also, the colemanite concrete and B_4C shielding give a good ability to reduce the radioactive wastes. As the aspect of the radiation shielding, hematite and magnetite concretes with #1 strategy and B_4C shielding material with #2 strategy give better performance compared to the other methods. These results can be used to select the shielding material and strategies for ISOL facility.

Acknowledgement

This work was supported in part by Project on Radiation Safety Analysis of RAON Accelerator Facilities grant funded by Institute for Basic Science (Project No.: 2013-C062) and Innovative Technology Center for Radiation Safety (iTRS).

REFERENCES

[1] J. K. Ahn, et al., Baseline Design Summary, Rare Isotope Science Project, IBS, August, 2012.
[2] D. H. KIM, and et al., A Preliminary Study on the Air and Concrete Activation Analysis for RAON ISOL-Bunker, Transactions of the Korean Nuclear Society, Pyeongchang, Korea, October 30-31, 2014.
[3] S. H. KIM, and et al., A Preliminary Study on the Prompt Radiation Shielding Analysis for Target Rooms in the RAON ISOL Facility, Transactions of the Korean Nuclear Society, Pyeongchang, Korea, October 30-31, 2014.
[4] T. ZAGAR, M. BOZIC, M. RAVNIK, Long-lived Activation Products in TRIGA Mark II Research Reactor Concrete Shield: Calculation and Experiment, Journal of Nuclear Materials, Vol. 335.3, P. 379-386, 2004.
[5] K. Masumoto, and et. al., Evaluation of Radioactivity Induced in the Accelerator Building and its Application to Decontamination Work. Journal of Radioanalytical and Nuclear Chemistry, Vol. 255.3, P. 465-469, 2003.
[6] G. Hampel, F. Scheller, W. Bernnat, and et. al., Calculation of the Activity Inventory for the TRIGA Reactor at the Medical University of Hannover (MHH) in Preparation for Dismantling the Facility, Waste Management 2002 Symposium, Feb 24-28, 2002, Tucson, AZ (US)
[7] B. Oto, and A. Gür, Gamma-ray Shielding of Concretes Including Magnetite in Different rate, International Journal of Physical Sciences, Vol. 8.8, P. 310-314, 2013.

[8] O. Gencel1, et al., An investigation on the concrete properties containing colemanite, International Journal of Physical Sciences, Vol. 5.3, P. 216-225, 2010.
[9] O. Gencel1, Gamma and neutron shielding characteristics of concretes containing different colemanite proportions, Nuclear Science and Technology, P. 41-49, 2012.
[10] C. Yixue, W. Yican, and U. Fischer, The Rigorous-2-step Calculation of Shutdown Dose Rates for Nuclear Fusion Devices, Nuclear Techniques, Vol.26, P. 763, 2003.
[11] D.B Pelowitz, editor, MCNPXTM User's Manual, Version 2.7.0, LA-CP -11-00438, Los Alamos National Laboratory, 2011.
[12] R. A. Forrest, FISPACT-2003 User Manual EASY 2003, UKAEA FUS, Vol. 485, 2003.
[13] D. H. KIM, and et al., An Activation Inventory Estimation Including Spallation Reactions by Modification of FISPACT 2010 Code, Transactions of the Korean Nuclear Society, Jeju, Korea, May 7-8, 2015.